Published May 11, 2017

Technical Notes

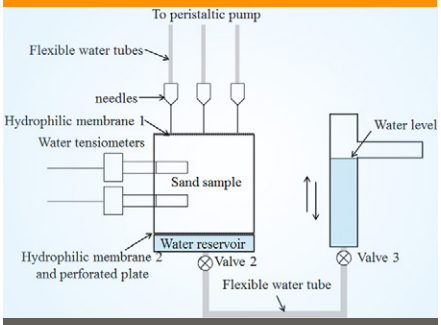


**Core Ideas**

- We devised a setup to measure hydraulic properties using the multistep flux method.
- Results showed good agreement with the data obtained with the hanging water column.
- However, they deviated slightly from independent data obtained with the HYPROP.

L. Zhuang, S.M. Hassanizadeh, and M.Th. van Genuchten, Dep. of Earth Sciences, Utrecht Univ., Princetonlaan 9, P.O. Box 80021, 3508 TA, Utrecht, the Netherlands; C.R. Bezerra Coelho, Dep. of Civil Engineering, COPPE, Federal Univ. of Rio de Janeiro, UFRJ, Rio de Janeiro, RJ, 21945-970, Brazil; S.M. Hassanizadeh, Soil and Groundwater Systems, Deltares, Princetonlaan 6, 3584 CB, Utrecht, the Netherlands; M.Th. van Genuchten, NIDES Interdisciplinary Center for Social Development, Federal Univ. of Rio de Janeiro, UFRJ, Rio de Janeiro, RJ, 21945-596, Brazil. *Corresponding author (S.M.Hassanizadeh@uu.nl).

Received 22 Nov. 2016.
Accepted 8 Mar. 2017.

Citation: Zhuang, L., C.R. Bezerra Coelho, S.M. Hassanizadeh, and M.Th. van Genuchten. 2017. Analysis of the hysteretic hydraulic properties of unsaturated soil. Vadose Zone J. 16(5). doi:10.2136/vzj2016.11.0115

Vol. 16, Iss. 5, 2017


# Analysis of the Hysteretic Hydraulic Properties of Unsaturated Soil

**L. Zhuang, C.R. Bezerra Coelho, S.M. Hassanizadeh,* and M.Th. van Genuchten**

Knowledge of the unsaturated soil hydraulic properties is essential for modeling water flow and solute transport processes in variably saturated subsurface systems. Various experimental setups have been developed over the years to measure the hydraulic properties. We devised a relatively simple setup for simultaneous measurement of the water retention and unsaturated hydraulic conductivity curves using multistep flux (MSF) and hanging water column (HWC) experiments. Our focus was especially on medium- and coarse-textured sands having relatively narrow particle-size distributions as reflected by the van Genuchten–Mualem (VGM) hydraulic parameter *n*. Values of the VGM parameter *n* for some of the sands we used were as high as 15. We also measured the hydraulic properties using the HYPROP evaporation method. The MSF and HWC results showed excellent agreement, but deviated slightly from independent data obtained with the HYPROP measurement system.

Abbreviations: HMS, HYPROP measurement system; HWC, hanging water column method; MSF, multistep flux method; VG, van Genuchten; VGM, van Genuchten–Mualem.

Quantifying the unsaturated soil hydraulic properties is essential to understanding and modeling fluid flow and contaminant transport in the vadose zone, as well as for other variably saturated multiphase flow systems. The constitutive relationships for air–water systems generally involve the water content, θ, as a function of the pressure head, $h$, and the hydraulic conductivity, $K$, as a function of the pressure head or water content. A range of laboratory methods have been developed over the years for estimating the soil hydraulic properties (cf. van Genuchten and Wierenga, 1986; van Genuchten et al., 1997; Dane and Hopmans, 2002; Durner and Lipsius, 2005). This includes not only direct measurement of θ and/or $K$ at specific pressure heads or water contents but also the use of inverse procedures to estimate the complete $\theta(h)$ and/or $K(\theta)$ curves (Durner et al., 1999; Hopmans et al., 2002).

Starting with the early studies by Becher (1971) and Wind (1968), the evaporation method is now widely used to estimate the water retention and the unsaturated hydraulic conductivity curves simultaneously. The method has seen many improvements over the years (e.g., Halbertsma, 1996; Wendroth et al., 1993; Peters and Durner, 2008; Schindler and Müller, 2006; Peters et al., 2015), leading to a semi-automated version (referred to here as the HYPROP measurement system, HMS) that is now being commercialized by Decagon Devices and UMS AG. The method uses values of the pressure head measured at two depths within a 5-cm soil sample, along with the weight of the soil sample during the evaporation process, to estimate the soil hydraulic data. While very reliable results have been reported for the HMS approach, one inherent drawback of evaporation methods is that the results hold only for the drainage branches of the soil hydraulic properties.

An alternative simultaneous direct approach is the multistep flux (MSF) method based on vertically uniform flow (Dirksen and Matula, 1994; Weller et al., 2011; Weller and Vogel, 2012; Kumahor et al., 2015). The method allows measurements of $K(h)$ assuming unit gradient conditions during steady-state downward flow in a soil column. Water inflow rates

are adjusted to achieve the same pressure heads when measured at two or more vertical positions. The fluid flow rate then becomes equal to $K$ at the measured $h$. Repeating the measurements at various flow rates and corresponding pressure heads will produce the desired hydraulic data points.

As part of this study, we constructed a relatively simple experimental setup using a small flow cell for measuring the unsaturated soil hydraulic properties. We measured the hysteretic properties of two soil samples having relatively narrow pore-size distributions and compared the results with the more standard multistep hanging water column (HWC) approach. The studies were motivated in part to have reliable soil hydraulic data for more theoretical studies of hysteresis phenomena using alternative thermodynamics-based interfacial area approaches (Zhuang, 2017). Moreover, relatively few experimental and numerical studies have been performed on sands characterized by relatively narrow particle-size distributions (e.g., Weller et al., 2011; Weller and Vogel, 2012; Mahmoodlu et al., 2016; Wang et al., 2016; Zhuang et al., 2016).

# Materials and Methods

## Sand Materials

We investigated two types of sands. One sand, S1, was obtained from a sand mining site (Sibelco) with particles ranging from 0.1 to 0.5 mm. The other sand (S2), having grain sizes between 0.1 and 1 mm, was obtained from a riverbed in the Netherlands. Prior to use, the two sandy soils were rinsed with deionized water and then air dried. Saturated hydraulic conductivities of the two samples were measured using a constant-head method (Reynolds et al., 2002) with the same sand cell holder as used for the multistep hanging water column and multistep flux experiments (Fig. 1). Selected properties of the two sand samples are shown in Table 1. The particle density was calculated based on the weight and volume of the sand particles. The sand volume was represented by the volume of water that overflowed when the sand particles were placed in degassed water. The measurements and calculations were repeated to obtain an average value of the particle density. Values of the average porosity were calculated using data from all experiments (HWC, MSF, and HMS).

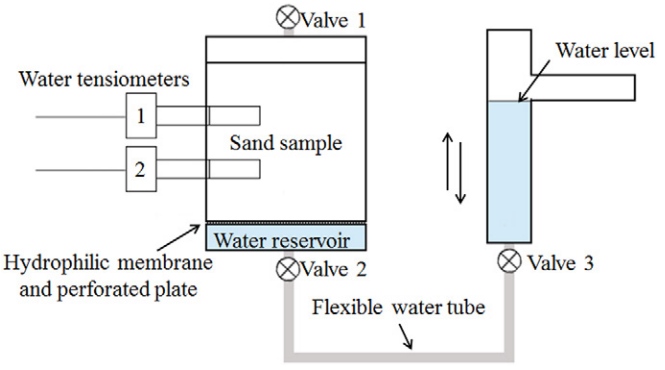


Fig. 1. Schematic view of the experimental setup for the hanging water column (HWC) experiments.

## Hanging Water Column Experiments

Figure 1 shows a schematic of our HWC experimental setup. A custom-built Plexiglas cell was used for the sand samples. The dimensions of the cell were 3 cm (height) by 3 cm (length) by 2 cm (width). A valve at the top of the sandbox (Valve 1) was connected to a balloon filled with moist air to keep constant atmospheric pressure. At the bottom of the sand cell, a 5-μm hydrophilic nylon membrane was held by a stainless-steel porous plate to serve as a capillary barrier. The water reservoir at the bottom of the setup was connected to a small hanging water column, which was used to control the pressure head at the outlet. Water in the small hanging column could overflow during drainage, while extra water was added to keep the water head in the column constant during imbibition. Silicone tape was used at all joints to avoid any leakage.

Two mini-tensiometers (Rhizo Instruments) were installed at depths of 1 and 2 cm in the sand sample cell. The tensiometers consisted of a ceramic cup, 1 cm long and 4 mm in diameter, and a small pore pressure transducer. An air-permeable but water-impermeable plastic hollow fiber was used to connect the ceramic cup to a vacuum to remove air from the tensiometers. Prior to use, the tensiometers were saturated with deionized water, while during the experiments, the tensiometers were always connected to an automatic vacuum system. This ensured that the tube between the ceramic cup and the transducer remained filled with water. The pressure transducers were connected to a CR1000 datalogger (Campbell Scientific). Tensiometer readings were collected every 1 min.

Water contents in the middle of the sand sample were measured using the γ-ray transmission method. When a beam of γ radiation passes through a sample of thickness $x$, the transmission of photons can be described using the Beer–Lambert law, which for an unsaturated soil sample can be written as

$$I = I_0 \exp\left(-\mu_s x_s - \mu_w x_w\right) \quad [1]$$

where $I$ and $I_0$ are the measured and corresponding reference intensities, respectively, $\mu_s$ and $\mu_w$ are the soil and water attenuation coefficients, respectively, and $x_s$ and $x_w$ denote path lengths of the γ-ray beam through soil and water, respectively. Values of the

Table 1. Properties of the two sands used in the experiments.

| Properties | S1 | S2 |
|---|---|---|
| Mean particle diameter ($d_{50}$), mm | 0.20 | 0.28 |
| Uniformity coefficient ($C_u$)† | 2.3 | 3.3 |
| Particle density ($\rho_s$), g cm$^{-3}$ | 2.56 | 2.55 |
| Saturated conductivity ($K_s$), cm h$^{-1}$ | 61.2 | 75.6 |
| Average porosity ($\varphi$) | 0.39 | 0.36 |

† $C_u$ is the ratio of $d_{60}$ to $d_{10}$.

porosity ($\varphi$) of the sand and its water content ($\theta$) can be calculated from $x_s$ and $x_w$ using

$$\varphi = \frac{x - x_s}{x} \quad \text{and} \quad \theta = \frac{x_w}{x} \qquad [2]$$

respectively, where $x$ is the total thickness of the soil sample (i.e., 2 cm, being the width of our experimental setup).

For our study we used a dual-energy $\gamma$-ray system. The $\gamma$-ray sources consisted of $^{241}$Am, with an energy peak of 59 keV, and $^{137}$Cs, with an energy peak of 662 keV. The diameter of the $\gamma$-ray beam was 6 mm. Measured intensities hence were average values across the cross-section of the beam and the sample thickness $x$.

The attenuation coefficients $\mu_s$ and $\mu_w$ for both $^{241}$Am and $^{137}$Cs were measured and calculated beforehand. Details of the calibration procedures and the dual $\gamma$-ray system were given by Fritz (2012). We chose the intensities of the empty cell as the reference $I_0$ for both $^{241}$Am and $^{137}$Cs. Intensities for $^{241}$Am and $^{137}$Cs can be collected simultaneously for each $\gamma$-ray transmission measurement, while $x_s$ and $x_w$ can be calculated from Eq. [1], written for Am and Cs separately. Once $x_s$ and $x_w$ are known, the sand porosity ($\varphi$) and water content ($\theta$) can be calculated for every $\gamma$-ray transmission measurement. Water contents were measured after equilibration of the soil sample at each imposed water level (and hence pressure head). During primary drainage, the total amount of water from the outlet at equilibrium was recorded every two or three elevations. The resulting average water contents were essentially identical to the measured water contents using $\gamma$-ray transmission.

The experimental setup was first mounted with the bottom reservoir and the cell full of water and without the top lid. Deionized and degassed water was used to minimize air entrapment. The cell was packed by pouring dry sand continuously into the water-filled cell through a funnel and regularly tapping the sand. A small comb was used to mix the sand in the water to avoid layering. The top cover was installed after packing the sand uniformly. All experiments were conducted in a constant-temperature room at 21 $\pm$ 0.5°C.

## Multistep Flux Experiments

We modified the HWC setup to enable also MSF experiments. This allowed us to measure unsaturated conductivities and the water retention curve directly. Water flow in the porous medium was described using the standard Darcy–Buckingham equation:

$$q = -K(\theta)\left(\frac{\partial h}{\partial z} - 1\right) \qquad [3]$$

where $q$ is the fluid flux and $z$ is vertical spatial coordinate. For unit gradient flow in the vertical direction (i.e., when $\partial h/\partial z$ = 0), the flux becomes equal to the hydraulic conductivity, $K(h)$. Different hydraulic conductivity values can be obtained by changing the inflow rate and the height of the hanging water column (and thus of $h$).

A sketch of the MSF experimental setup is shown in Fig. 2. Six injection needles (two in the lateral direction and three in the longitudinal direction) were used to obtain a spatially uniform water inflow rate to the top of the cell. Each needle was connected to a tube with an inner diameter of 2 mm. The six tubes were connected to a peristaltic pump that controlled the injected flow rate. The tips of needles were put in contact with a 200-µm hydrophilic nylon membrane (Hydrophilic Membrane 1 in Fig. 2) to establish a homogenous water flow rate into the sand sample.

A series of continuous water flow conditions were established during the various experiments, i.e., starting from primary drainage, to scanning imbibition, and then to main drainage. After packing the saturated sand samples into the cell, a water flow rate, slightly smaller than the measured saturated hydraulic conductivity (as obtained with the constant-head method), was applied to the top of the sample. The hanging water column was then kept at the same level as the bottom of the sand sample.

Readings of the two tensiometers were collected continuously, while outflow was measured when the readings of the two tensiometers became identical, in which case the measured outflow was assumed to be equivalent to the value of the hydraulic conductivity at the pressure head obtained from the tensiometer readings. The process was reversed when the water flow rate became too small for the peristaltic pump. The level of the hanging column after each step was moved to a new elevation prior to decreasing the flow rate using the pump during drainage, while moving in the opposite manner during imbibition using higher flow rates. The level of the hanging column at each step was first estimated from the HWC experiments and then adjusted every 0.5 or 1 cm based on the difference between the two tensiometer readings. The water content

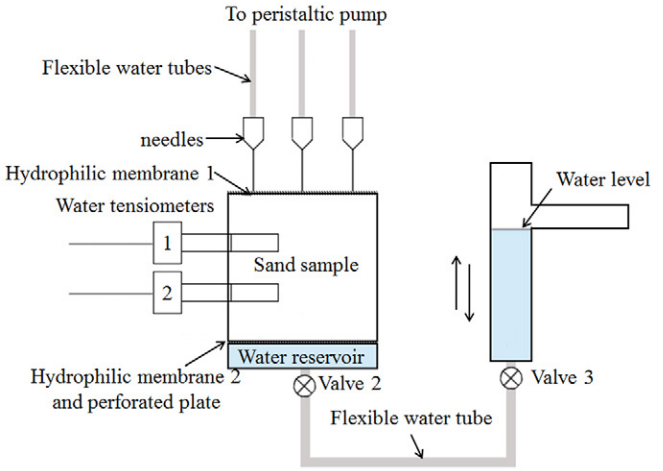


Fig. 2. Schematic view of the experimental setup for the multistep flux (MSF) experiments.

in the middle of the sample was measured once the tensiometer readings had stabilized.

## HYPROP Experiments

We used the HYPROP commercial device (UMS AG) to carry out the HMS evaporation experiments. Saturated soil samples (250 $cm^3$, 5 cm in height) were prepared for this purpose following the HYPROP manual. Dry sand was first placed in the sample rings, which were then put into distilled and degassed water. The soil samples were saturated with water from the bottom through a porous plate. Once saturated, the soil samples were sealed at the bottom and exposed at the top for evaporation. Values of the pressure head were monitored continuously at two depths (1.25 and 3.75 cm). The weight loss of the sample was measured simultaneously so that values of the water content could be calculated volumetrically. At any given time, values of the water content, the pressure head, and the unsaturated hydraulic conductivity were calculated using the HYPROP-FIT software as documented by Pertassek et al. (2015). The software uses geometric mean values of the pressure heads measured with the two tensiometers.

## Soil Hydraulic Functions

Measured soil water retention and unsaturated conductivity data were analyzed in terms of the van Genuchten–Mualem (VGM) equations (van Genuchten, 1980):

$$\theta(h)=\theta_r+\frac{\theta_s-\theta_r}{\left(1+|\alpha h|^n\right)^m} \quad [4]$$

$$K(\theta)=K_s(S_e)^l\left[1-\left(1-S_e^{1/m}\right)^m\right]^2 \quad [5]$$

$$S_e=\frac{\theta-\theta_r}{\theta_s-\theta_r} \quad [6]$$

where $\theta_s$ and $\theta_r$ are the saturated and residual water contents, respectively; $S_e$ is the effective saturation, $K_s$ is the saturated hydraulic conductivity; $\alpha$, $n$, and $l$ are fitting parameters; and $m = 1 - 1/n$. All optimizations of the retention data were performed using the RETC software (van Genuchten et al., 1991).

# Results and Discussion

Three replicates were conducted for all experiments. Because of the very close overlap of the replicates, only one measurement set is shown here for each sand.

## Hanging Water Column Experiments

While the HWC experiments for Sands S1 and S2 each lasted approximately 2 wk, the exact duration depended on the number of elevations and the times needed to reach equilibrium. Typical equilibration times at early and later stages for primary drainage for Sand S1 are shown in Fig. 3. The top of the soil sample was taken as a reference for the level of the hanging water column. As can be seen, the equilibration times were very short initially but then increased because of lower conductivities when the sample dried out.

Water retention data for the two sands as obtained with the HWC experiments are shown in Fig. 4a and 4b. The different symbols represent the HWC measured retention data during primary drainage, main imbibition, and main drainage. The shapes of the retention curves are consistent with the particle-size distribution ranges of the two sands: the retention curve of Sand S1 with its narrow particle-size distribution range is flatter for both drainage and imbibition.

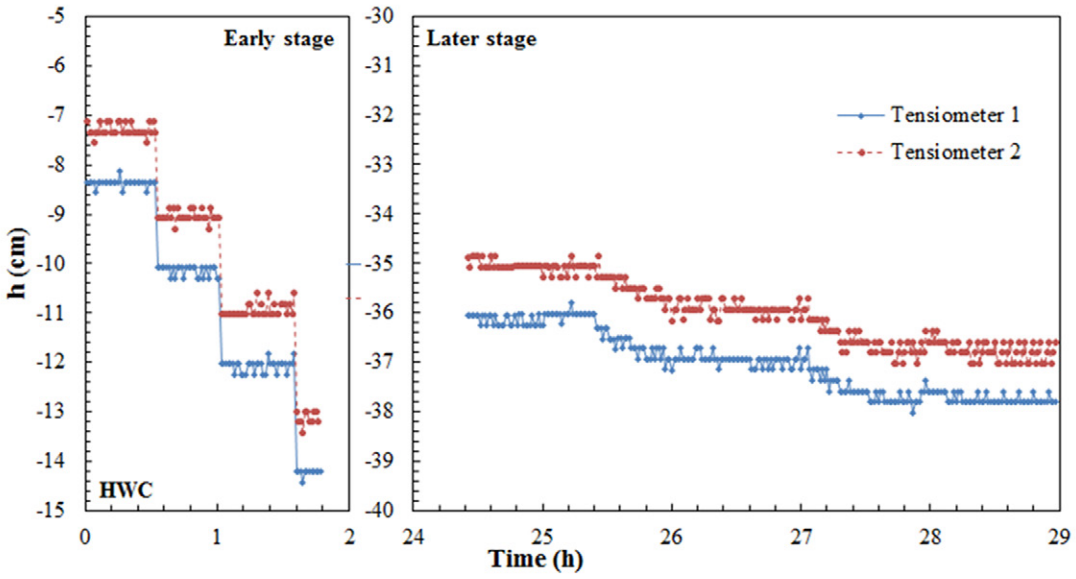


Fig. 3. Hanging water column experiments: typical trajectories of the two tensiometer readings for primary drainage for Sand S1.

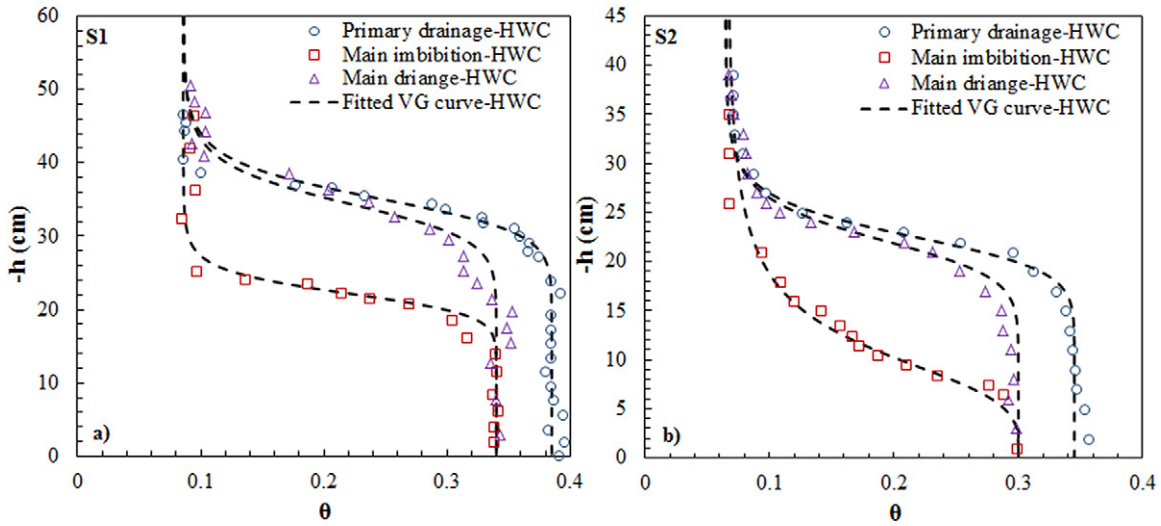


Fig. 4. Hanging water column (HWC) experiments: water retention data for Sands S1 and S2, together with the fitted van Genuchten (VG) water retention curves.

Figure 4 also includes the van Genuchten (VG) retention functions (dashed lines) as fitted to the experimental data. The fitted parameter values are listed in Table 2. The residual water content $\theta_r$ was fitted iteratively, using RETC, to the same value for each sand for all HWC experiments. The fitted value of the saturated water content $\theta_s$ for the main drainage and imbibition curves was less than the porosity due to air entrapment (leading to a non-zero residual air content).

Table 2. Values of the fitted van Genuchten–Mualem hydraulic parameters for the different experiments.

| Experiment† | $\alpha$ | $n$ | $\theta_r$ | $\theta_s$ | $K_s$ | $l$ |
|---|---|---|---|---|---|---|
| | $cm^{-1}$ | | —$cm^3\ cm^{-3}$— | | cm $h^{-1}$ | |
| Sand S1 | | | | | | |
| Primary drainage, HWC | 0.0284 | 14.5 | 0.086 | 0.385 | – | – |
| Main imbibition, HWC | 0.0451 | 14.8 | 0.086 | 0.340 | – | – |
| Main drainage, HWC | 0.0288 | 13.5 | 0.086 | 0.340 | – | – |
| Primary drainage, MSF | 0.0315 | 15.1 | 0.087 | 0.385 | 61.2 | 0.81 |
| Scanning imbibition, MSF | 0.0553 | 8.0 | 0.110 | 0.340 | 41.0 | 0.40 |
| Main drainage, MSF | 0.0322 | 10.0 | 0.086 | 0.340 | 41.0 | 0.82 |
| Primary drainage, HMS | 0.0219 | 10.0 | 0.068 | 0.410 | 61.2 | 0.20 |
| Sand S2 | | | | | | |
| Primary drainage, HWC | 0.0442 | 12.2 | 0.065 | 0.345 | – | – |
| Main imbibition, HWC | 0.1003 | 3.9 | 0.065 | 0.300 | – | – |
| Main drainage, HWC | 0.0453 | 11.1 | 0.065 | 0.300 | – | – |
| Primary drainage, MSF | 0.0460 | 12.2 | 0.065 | 0.338 | 75.6 | 4.50 |
| Scanning imbibition, MSF | 0.1007 | 4.0 | 0.141 | 0.300 | 22.0 | −0.50 |
| Main drainage, MSF | 0.0480 | 10.0 | 0.065 | 0.300 | 22.0 | 2.00 |
| Primary drainage, HMS | 0.0421 | 5.9 | 0.044 | 0.363 | 75.6 | 0.66 |

† HWC, hanging water column; MSF, multistep flux; HMS, HYPROP measuring system.

## Multistep Flux Experiments

The MSF experiments for the two sands each lasted about 10 d. Typical pressure head changes from one uniform condition to another uniform condition for primary drainage during the MSF experiments are shown in Fig. 5. The level of the hanging column was always kept lower than the tensiometer readings during primary drainage. When the inflow rate was reduced, initially a relatively large difference between the two tensiometer readings could be observed. After stabilization of the tensiometer readings, the level of the hanging column was lowered carefully in small steps (every 0.5 cm) until the readings of two tensiometers became the same, thus reflecting steady-state conditions.

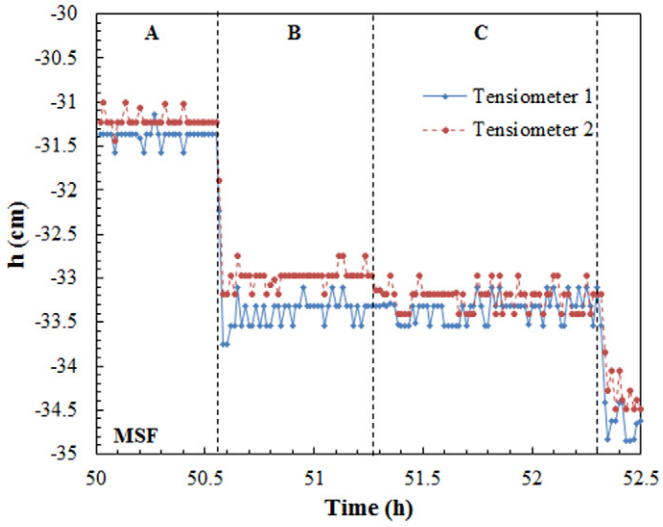


Fig. 5. Multistep flux (MSF) experiments: typical trajectories of the two tensiometer readings for primary drainage for Sand S1: (A) inflow rate of 13.7 cm $h^{-1}$ and a hanging water level of −37 cm; (B) inflow rate of 6.8 cm $h^{-1}$ and a hanging water level of −37 cm; (C) inflow rate of 6.8 cm $h^{-1}$ and a hanging water level of −37.5 cm.

Figures 6a and 6b show observed water retention data for the two sands as measured using the MSF experiments. Different symbols are used for the primary drainage, scanning imbibition, and main drainage data points. Fitted VGM curves for the MSF experiments are shown as solid lines. Also included for comparison are the fitted VG curves of the HWC experiments (dashed lines; the same curves as in Fig. 4). Both sands showed reasonable consistency in terms of the HWC and MSF retention data, especially considering that the imbibition branches of the HWC data presented main imbibition, while the MSF imbibition branch represented a scanning curve. The retention curves of Sand S1 obtained with the MSF method is situated slightly below the HWC data for both drainage and imbibition. A minor rearrangement of small sand particles during the MSF experiments may have contributed to the discrepancies, as perhaps the presence of some nonequilibrium dynamic effects (e.g., Weller et al., 2011; Diamantopoulos and Durner, 2012).

Unsaturated hydraulic conductivities obtained using the MSF method are shown in Fig. 6c and 6d. The conductivity vs. water content data showed very little or no hysteresis between the main drainage, primary wetting, and main wetting branches, consistent with previous studies (e.g., Poulovassilis, 1969; Tzimas, 1979). The unsaturated conductivities of the two sands at high water contents were close to the saturated conductivity as measured with the constant-head method.

We used the VGM model to obtain a simultaneous fit of the MSF measured water retention and unsaturated conductivity data. The resulting curves are shown as solid lines in Fig. 6. Values of the residual water content, $\theta_r$, for primary and main drainage were fixed at those obtained with the HWC experiments, while its value was fitted for the scanning imbibition curve. The value of the saturated conductivity $K_s$ for primary drainage was taken to be the value measured using the constant-head method. The value of $K_s$ for primary drainage was taken to be the value measured using the constant-head method, while $K_s$ for the scanning and main drainage branches was fixed at the largest measured value obtained for these two branches. The estimated values are shown

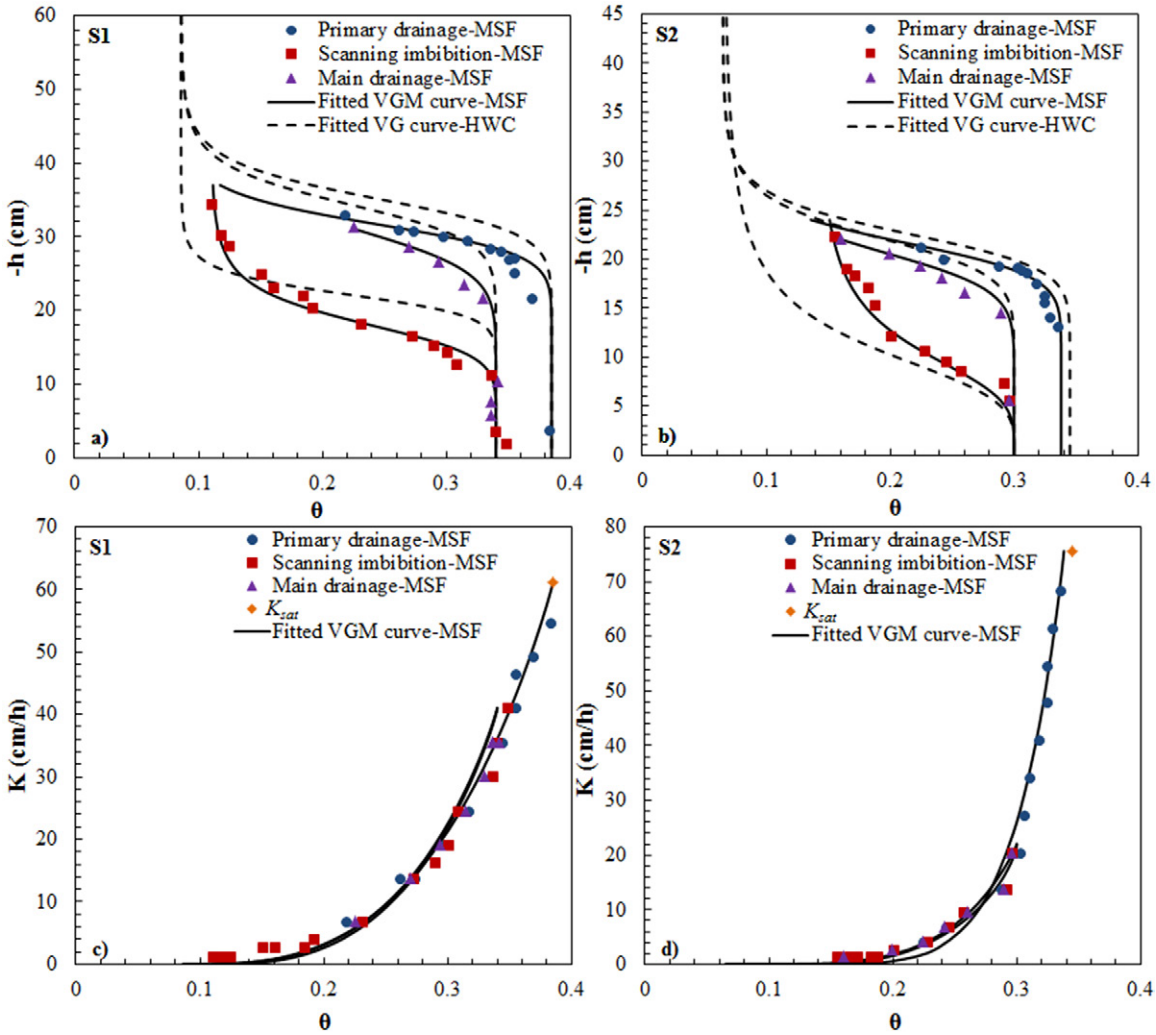


Fig. 6. Multistep flux (MSF) experiments: water retention data, including the fitted van Genuchten–Mualem (VGM) curve for the MSF experiments and the fitted van Genuchten (VG) curve for the hanging water column (HWC) experiments for comparison (top), and unsaturated hydraulic conductivities, including the saturated hydraulic conductivity ($K_{sat}$) and the fitted VGM curve (bottom) for Sands S1 and S2.

in Table 2. Small differences in the fitting parameter values existed between the HWC and MSF data points for primary and main drainage. Values of the pore connectivity parameter *l* showed some variation among the various curves. However, fixing the value at 0.5 as suggested by Mualem (1976) did not have a major effect on the plotted curves, except for the MSF primary drainage and scanning imbibition curves of Sands S1 and S2 (results not further shown here). This was not overly surprising because many (not all) of the soils used in the analysis by Mualem were also relatively coarse-textured disturbed porous media as in our study. Values of *l* for other soils often deviate significantly from 0.5 (e.g., Yates et al., 1992; Schaap and Leij, 2000).

## Comparison with HYPROP Evaporation Data

We compared some of the HWC and MSF primary drainage data with the HYPROP (HMS) evaporation experiments. Figures 7a and 7b show that the HMS setup produced very well-defined smooth retention curves but with somewhat higher saturated water contents than the HWC data, as well as lower residual water contents. The primary drainage curve for Sand S1 obtained with the HMS evaporation method was situated above the curve obtained with the HWC method throughout the entire water content range (Fig. 7a), while the data for Sand S2 showed only slight differences, mostly in the drier water content range. Similar discrepancies between HMS data and especially pressure plate data were also noted by Schelle et al. (2013) for their coarse-textured samples. They offered three possible explanations for the deviations. One could be the different saturated water contents of the sand samples used for the two methods. Another possibility may be cooling effects during the evaporation experiments. The tensiometer readings are temperature dependent, which could have caused the measured retention curve to be shifted slightly upward (to larger absolute pressure head values). A third explanation could be possible dynamic nonequilibrium effects during the evaporation experiments, as discussed by Hassanizadeh et al. (2002) and Diamantopoulos and Durner (2012), among others. We conclude that more studies of the observed differences may be needed.

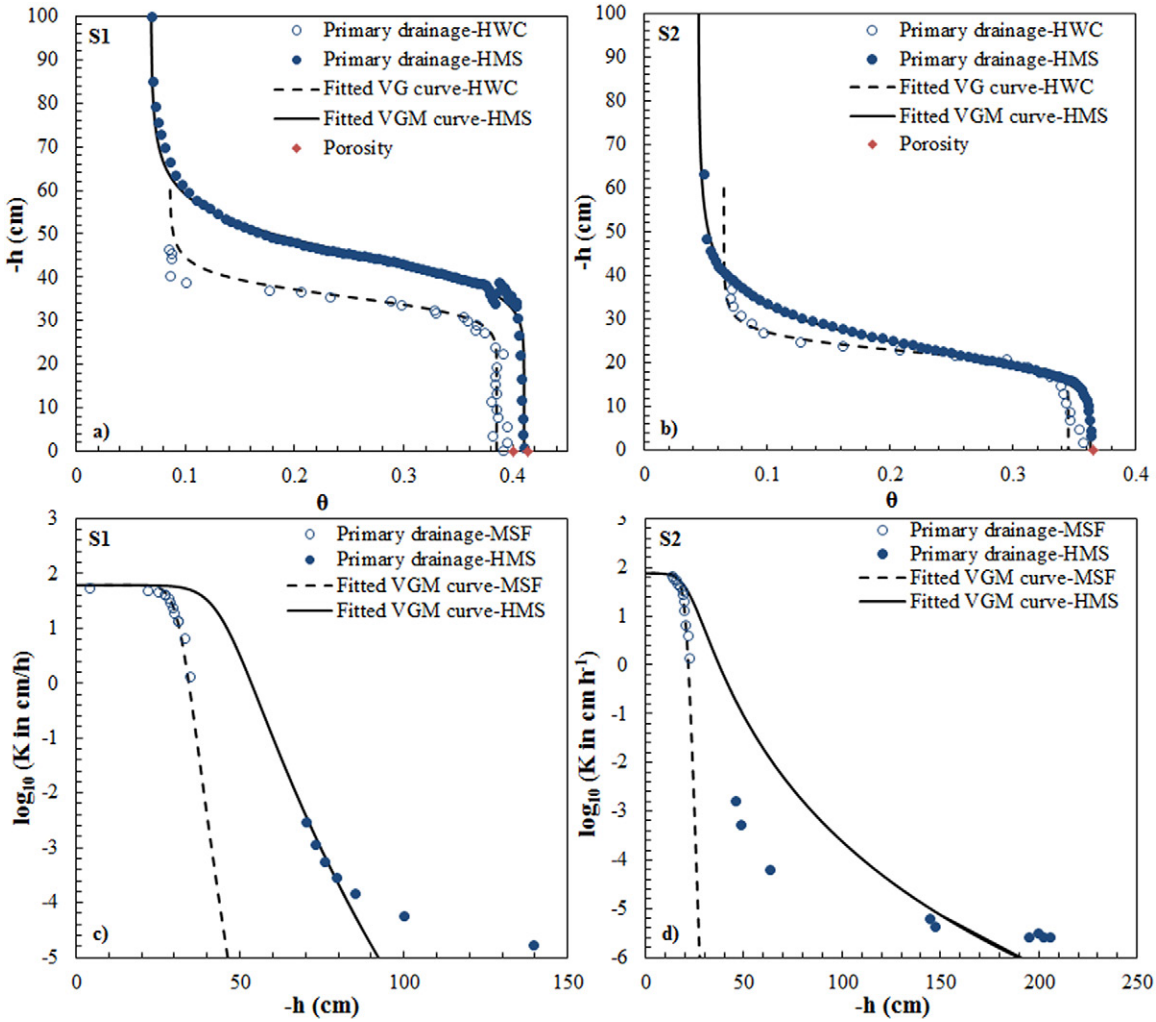


Fig. 7. Hanging water column (HWC) and HYPROP measuring system (HMS) experiments: measured and fitted van Genuchten–Mualem (VGM) and van Genuchten (VG) water retention data (top) and unsaturated hydraulic conductivity (bottom) curves during primary drainage of the HWC and multistep flux (MSF) experiments for Sands S1 (left) and S2 (right).

Unsaturated conductivities obtained with the MSF and HMS evaporation experiments are shown in Fig. 7c and 7d. Values of the unsaturated conductivity in this case are presented using a logarithmic scale. Results indicate a several orders of magnitude difference between the measured unsaturated hydraulic conductivities using the two methods. Unsaturated conductivity data points obtained with the evaporation method were mainly in the dry range, while MSF experiments measured unsaturated conductivities mainly in the wet range. Our results are consistent with other studies showing that HMS applications to soils having very narrow pore-size distributions (as reflected by van Genuchten $n$ values above 5 or even 10) may still produce reliable results for water retention but not for near-saturated hydraulic conductivity values (Peters et al., 2015).

Figure 7 includes the fitted VGM curves for the MSF and HMS measured soil water retention and hydraulic conductivity data. Fitted parameter values are reported in Table 2. Values of the saturated conductivity, $K_s$, of the two sands were fixed at those measured using the constant-head method. The fitted curves for the HMS data are indicated by solid lines in Fig. 7. They showed excellent agreement with the retention data but not with the unsaturated conductivity measurements. The HWC experiments produced mostly higher values of the parameters $\alpha$, $n$, and $\theta_r$ than the HMS experiments. We have included the measured file of one of the sands (S1) as supplemental material.

We conclude by noting that some of the differences between the HWC, MSF, and evaporation experiments may have been due to differences in the measured water contents caused by different averaging volumes. Water contents during the HWC and MSF experiments were measured using $\gamma$ transmission, in which case they were calculated based on the average volume of the $\gamma$ source opening area (6 mm in diameter) and the sample width (2 cm). By comparison, water contents during the evaporation experiments were averaged based on the entire volume of the sample rings (250 $cm^3$, 5 cm in depth). Moreover, due to the narrow particle-size distributions (especially for Sand S1), the moisture front during evaporation becomes very sharp, leading to large differences between the water contents in the upper and lower parts of the sample. This may cause the measured retention curve to be shifted slightly rightward at lower water contents. Such a situation may compromise the linearization assumptions inherent in the HMS evaporation approach (Peters et al., 2015).

## Concluding Remarks

In this study, we used three laboratory methods to characterize the unsaturated soil hydraulic properties of two sands having relatively narrow particle-size distributions. A small custom-built cell or box was developed to conduct HWC and MSF experiments, while the commercial HYPROP system was used for the evaporation experiments. Both drainage and imbibition curves could be obtained using the HWC and MSF methods. The HMS method, on the other hand, provides only primary drainage curves. The hysteretic retention data obtained with the HWC and MSF experiments showed good agreement with each other for the primary drainage and main imbibition processes. The MSF-measured unsaturated conductivities did not show distinct hysteretic behavior as a function of water content in that values for primary drainage, scanning imbibition, and main drainage all showed very little difference when plotted vs. the water content.

We also compared the HWC- and MSF-measured hydraulic data with the HMS evaporation results. Some discrepancies were found between the HWC and HMS retention data, presumably because of the assumed linear distribution of the water content vs. depth in the HMS approach. This assumption may not be valid for our porous media with very narrow particle-size distributions. Unsaturated conductivities using the HMS evaporation experiments were furthermore confined to the very dry range. Independent saturated conductivity measurements hence may be critical to obtain a good description of the complete hydraulic conductivity curve. Additional numerical and experimental studies may be needed to further clarify these issues.

### Acknowledgments

Author L. Zhuang would like to thank the China Scholarship Council (no. 201206380076) for financial support; S.M. Hassanizadeh has received funding from the European Research Council under the European Union's Seventh Framework Program (FP/2007-2013)/ERC Grant Agreement no. 341225. We would like to thank Associate Editor Peter Lehmann and two anonymous reviewers for providing constructive comments to the manuscript.

## References

Becher, H.H. 1971. Ein Verfahren zur Messung der ungesättigten Wasserleitfähigkeit. Z. Pflanzenernaehr. Bodenkd. 128:1–12. doi:10.1002/jpln.19711280102

Dane, J.H., and J.W. Hopmans. 2002. Water retention and storage: Laboratory. In: J.H. Dane and G. Topp, editors, Methods of soil analysis. Part 4. Physical methods. SSSA Book Ser. 5. SSSA, Madison, WI. p. 675–720. doi:10.2136/sssabookser5.4.c25

Diamantopoulos, E., and W. Durner. 2012. Dynamic nonequilibrium of water flow in porous media: A review. Vadose Zone J. 11(3). doi:10.2136/vzj2011.0197

Dirksen, C., and S. Matula. 1994. Automatic atomized water spray system for soil hydraulic conductivity measurements. Soil Sci. Soc. Am. J. 58:319–325. doi:10.2136/sssaj1994.03615995005800020009x

Durner, W., and K. Lipsius. 2005. Determining soil hydraulic properties. In: M.G. Anderson and J.J. McDonnell, editors, Encyclopedia of hydrological sciences. John Wiley & Sons, Chichester, UK. p. 1121–1144.

Durner, W., B. Schultze, and T. Zürmuhl. 1999. State-of-the-art in inverse modeling of inflow/outflow experiments. In: M.Th. van Genuchten et al., editors, Characterization and measurement of the hydraulic properties of unsaturated porous media. Part 1. Univ. of California, Riverside. p. 661–682.

Fritz, S. 2012. Experimental investigations of water infiltration into unsaturated soil: Analysis of dynamic capillarity effects. M.S. thesis. Stuttgart Univ., Stuttgart, Germany.

Halbertsma, J. 1996. Wind's evaporation method: Determination of the water retention characteristics and unsaturated hydraulic conductivity of soil samples; possibilities, advantages and disadvantages. In: Extended abstracts: European workshop on advanced methods to determine hydraulic properties of soils, Thurnau, Germany. 10–12 June 1996. Dep. of Hydrology, Univ. of Bayreuth, Bayreuth, Germany. p. 55–58.

Hassanizadeh, S.M., M.A. Celia, and H.K. Dahle. 2002. Dynamic effect in the capillary pressure-saturation relationship and its impacts on unsaturated flow. Vadose Zone J. 1:38–57. doi:10.2136/vzj2002.3800

Hopmans, J.W., J. Šimůnek, N. Romano, and W. Durner. 2002. Simultaneoud determination of water transmission and retention properties: Inverse methods. In: J.H. Dane and G.C. Topp, editors, Methods of soil analysis. Part 4. Physical methods. SSSA Book Ser. 5. SSSA, Madison, WI. p. 963–1008. doi:10.2136/sssabookser5.4.c40

Kumahor, S.K., G.H. de Rooij, S. Schlüter, and H.-J. Vogel. 2015. Water flow and solute transport in unsaturated sand: A comprehensive experimental approach. Vadose Zone J. 14(2). doi:10.2136/vzj2014.08.0105

Mahmoodlu, M.G., A. Raoof, T. Sweijen, and M.Th. van Genuchten. 2016. Effects of sand compaction and mixing on pore structure and the unsaturated soil hydraulic properties. Vadose Zone J. 15(8). doi:10.2136/vzj2015.10.0136

Mualem, Y. 1976. A new model for predicting the hydraulic conductivity of unsaturated porous media. Water Resour. Res. 12:513–522. doi:10.1029/WR012i003p00513

Pertassek, T., A. Peters, and W. Durner. 2015. HYPROP-FIT software user's manual, V.3.0. UMS AG, München, Germany.

Peters, A., and W. Durner. 2008. Simplified evaporation method for determining soil hydraulic properties. J. Hydrol. 356:147–162. doi:10.1016/j.jhydrol.2008.04.016

Peters, A., S.C. Iden, and W. Durner. 2015. Revisiting the simplified evaporation method: Identification of hydraulic functions considering vapor, film and corner flow. J. Hydrol. 527:531–542. doi:10.1016/j.jhydrol.2015.05.020

Poulovassilis, A. 1969. The effect of hysteresis of pore-water on the hydraulic conductivity. J. Soil Sci. 20:52–56. doi:10.1111/j.1365-2389.1969.tb01553.x

Reynolds, W.D., D.E. Elrick, E.G. Youngs, A. Amoozegar, H.W.G. Booltink, and J. Bouma. 2002. Saturated and field-saturated water flow parameters. In: J.H. Dane and G. Topp, editors, Methods of soil analysis. Part 4. Physical methods. SSSA Book Ser. 5. SSSA, Madison, WI. p. 797–801. doi:10.2136/sssabookser5.4.c30

Schaap, M.G., and F.J. Leij. 2000. Improved prediction of unsaturated hydraulic conductivity with the Mualem–van Genuchten model. Soil Sci. Soc. Am. J. 64:843–851. doi:10.2136/sssaj2000.643843x

Schelle, H., L. Heise, K. Jänicke, and W. Durner. 2013. Water retention characteristics of soils over the whole moisture range: A comparison of laboratory methods. Eur. J. Soil Sci. 64:814–821. doi:10.1111/ejss.12108

Schindler, U., and L. Müller. 2006. Simplifying the evaporation method for quantifying soil hydraulic properties. J. Plant Nutr. Soil Sci. 169:623–629. doi:10.1002/jpln.200521895

Tzimas, E. 1979. The measurement of soil-water hysteretic relationships on a soil monolith. Eur. J. Soil Sci. 30:529–534. doi:10.1111/j.1365-2389.1979.tb01006.x

van Genuchten, M.Th. 1980. A closed-form equation for predicting the hydraulic conductivity of unsaturated soils. Soil Sci. Soc. Am. J. 44:892–898. doi:10.2136/sssaj1980.03615995004400050002x

van Genuchten, M.Th., F.J. Leij, and L. Wu. 1997. Characterization and measurement of the hydraulic properties of unsaturated porous media (Parts 1 and 2). Univ. of California, Riverside.

van Genuchten, M.Th., F.J. Leij, and S.R. Yates. 1991. The RETC code for quantifying the hydraulic functions of unsaturated soils. Rep. EPA/600/2-91/065. R.S. Kerr Environ. Res. Lab., USEPA, Ada, OK. https://www.pc-progress.com/en/Default.aspx?retc.

van Genuchten, M.Th., and P.J. Wierenga. 1986. Solute dispersion coefficients and retardation factors. In: A. Klute, editor, Methods of soil analysis. Part 1. Physical and mineralogical methods. 2nd ed. SSSA Book Ser. 5. SSSA and ASA, Madison, WI. p. 1025–1054. doi:10.2136/sssabookser5.1.2ed.c44

Wang, H., T.K. Tokunaga, J. Wan, W. Dong, and Y. Kim. 2016. Capillary pressure–saturation relations in quartz and carbonate sands: Limitations for correlating capillary and wettability influences on air, oil, and supercritical $CO_2$ trapping. Water Resour. Res. 52:6671–6690. doi:10.1002/2016WR018816

Weller, U., O. Ippisch, M. Köhne, and H.-J. Vogel. 2011. Direct measurement of unsaturated conductivity including hydraulic nonequilibrium and hysteresis. Vadose Zone J. 10:654–661. doi:10.2136/vzj2010.0074

Weller, U., and H.-J. Vogel. 2012. Conductivity and hydraulic nonequilibrium across drainage and infiltration fronts. Vadose Zone J. 11(3). doi:10.2136/vzj2011.0134

Wendroth, O., W. Ehlers, H. Kage, J.W. Hopmans, J. Halbertsma, and J.H.M. Wösten. 1993. Reevaluation of the evaporation method for determining hydraulic functions in unsaturated Soils. Soil Sci. Soc. Am. J. 57:1436–1443. doi:10.2136/sssaj1993.03615995005700060007x

Wind, G.P. 1968. Capillary conductivity data estimated by a simple method. In: P.E. Rijtema and H. Wassink, editors, Water in the unsaturated zone. Vol. 1. Proceedings of the Wageningen Symposium. June 1966. Int. Assoc. Sci. Hydrol., Gentbrugge, Belgium. p. 181–191.

Yates, S.R., M.Th. van Genuchten, A.W. Warrick, and F.J. Leij. 1992. Analysis of measured, predicted, and estimated hydraulic conductivity using the RETC computer program. Soil Sci. Soc. Am. J. 56:347–354. doi:10.2136/sssaj1992.03615995005600020003x

Zhuang, L. 2017. Advanced theories of water infiltration and redistribution in porous media; experimental studies and modeling. Ph.D. diss. Utrecht Univ., Utrecht, the Netherlands.

Zhuang, L., S.M. Hassanizadeh, M.Th. van Genuchten, A. Leijnse, A. Raoof, and C. Qin. 2016. Modeling of horizontal water redistribution in an unsaturated soil. Vadose Zone J. 15(3). doi:10.2136/vzj2015.08.0109